Applied Scientific Research **59:** 141–158, 1998.

Planktonic Communities and Chaotic Advection in Dynamical Models of Langmuir Circulation

M.A. BEES
Mathematics Institute, University of Warwick, Coventry CV4 7AL, U.K.; and Ecosystems Analysis and Management Group, Department of Biological Sciences, University of Warwick, Coventry CV4 7AL, U.K.

Abstract. A deterministic mechanism for the production of plankton patches within a typical medium scale oceanic structure is proposed and investigated. By direct numerical simulation of a simple model of Langmuir circulation we quantify the effects of unsteady flows on planktonic communities and demonstrate their importance. Two qualitatively different zones within the flow are identified: chaotic regions that help to spread plankton and locally coherent regions, that do not mix with the chaotic regions and which persist for long periods of time. The relative importance of these regions to both phytoplankton and zooplankton is investigated, taking into account variations in plankton buoyancy. In particular, species-specific retention zone structure is discussed in relation to variations in environmental forcing.

Key words: plankton, mixing, resonant retention zones, patchiness, Langmuir circulation, chaotic advection.

1. Introduction

A mechanism for generating patchiness in systems of advected, buoyant particles is presented in this paper that employs a deterministic near-integrable flow field. Recent studies of plankton dynamics [14, 31, 33, 44] identify plankton patchiness as a possible cause of the discrepancies between predictions from bulk-averaged models and field measurements. In particular, local aggregations of planktonic species are sometimes observed entrained in larger scale circulations [14, 15, 29, 39]. These "patches" of phytoplankton can persist for long periods of time irrespective of the apparently strong diffusive or mixing processes characteristic of turbulent flows. This description does not explicitly include turbulence or any stochastic forcing but their possible effects are discussed.

We choose Langmuir circulation in a stably-stratified fluid, a typical medium-scale structure, to demonstrate our approach in detail. Langmuir circulations [19] are formed by a balance between a destabilizing, wind induced, Stokes drift gradient and a stabilizing, temperature driven, vertical density stratification [10]. The resulting long roll structures can be identified from the debris at regions of surface convergence, called windrows, that occur between 2 and 200 m apart (see [2];

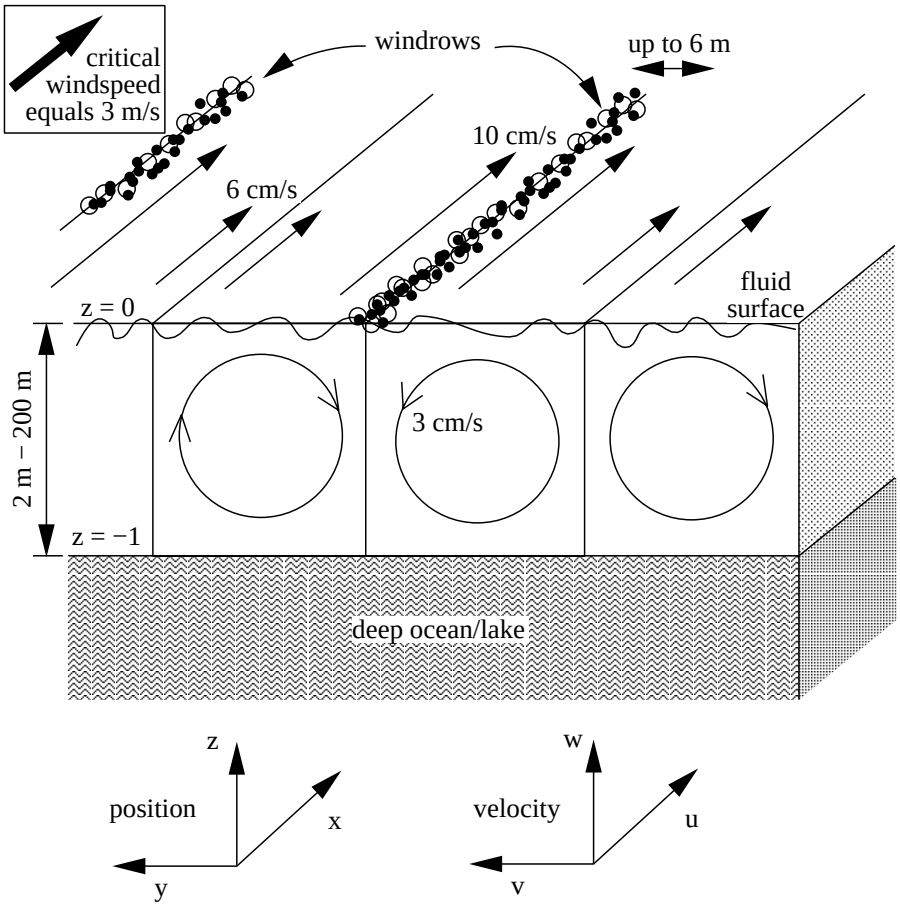

Figure 1. Coordinate system and representation of the steady flow. Typical field measurements, as discussed by [2, 21], are indicated.

Figure 1). Rather than track planktonic motion in Langmuir circulation experimentally, we choose instead to simulate a mathematical flow field, that can be directly controlled. Plankton are inserted into the flow and their trajectories are recorded. We insist that the plankton can do no more than swim up or down (effectively modelled as buoyancy). Hence, we are able to study the effect of the flow on the plankton without getting distracted by other physical or biological factors.

Craik and Leibovich [10] first derived a successful physical model of Langmuir circulation that has subsequently been used to generate a reduced-dimensional system [26]. These authors have investigated the bifurcational structure of Langmuir circulation, employing methods from dynamical systems, and have identified both steady and unsteady flow regimes. We will use this reduced model in our description but impose an additional time-dependent perturbation. The particular perturbation that we will use, whilst being physically realisable, is somewhat arbitrary and similar results can be obtained with other perturbations. However, we

wish to highlight our qualitative arguments and interpretations with quantitative results.

Chaotic advection is a fashionable mechanism for the deterministic transport of scalars that is independent of molecular diffusion [7, 18]. Unsteady or quasi-steady flows can exhibit non-integrable dynamics that can induce transport of advected scalars across what would normally be impenetrable barriers (or equivalently streamsurfaces) for steady integrable flows [1]. Small time-dependent perturbations to steady flows can break up these barriers and produce an "effective diffusivity" for purely advected scalars. The resulting lobe dynamics [40] for heteroclinic connections in Langmuir circulation may describe important cell-to-cell mixing processes. In the biological literature, Langmuir circulation has long been thought to play a significant role in causing planktonic mixing and/or patchiness (e.g., Stommel retention zones; [35, 36]). The mechanism described here is likely to work in addition to other patch-forming mechanisms, such as reaction-swimming-diffusion [3, 4, 11] and reaction-advection-diffusion [23, 24, 34] but tends to work on shorter timescales. Typically, patterns can form in hours over lengthscales of hundreds of meters.

This study aims to highlight some mechanisms for the production of plankton patches and to investigate their implications on planktonic communities. In particular, we wish to illustrate how a very small level of physical forcing can dramatically affect the interactions within an ecosystem. We concentrate on simulating the trajectories of individual plankton, in a Lagrangian sense, in order to understand how their strategies may enable them to aggregate and disperse. In this paper we use simulations as a tool in order to discuss, and perhaps answer, the following questions:

1. In what manner does chaotic advection help to disperse and/or concentrate plankton? What are the effects of buoyancy on the cross-sectional phytoplankton distribution and does buoyancy offer any strategic advantages?
2. How do zooplankton minimize their foraging time (or effort) and, hence, maximise their growth in an unsteady flow field? Should predators "do as the prey do", or is there a better strategy to find food in unsteady flows?
3. Does plankton patchiness persist in changing environmental conditions? What would be the effects of daily cycles of light, temperature and forcing frequency variations on Langmuir circulations, and what consequences do these have for plankton patchiness and their dynamics?

The key mathematical features of the model are described in Section 2 and some results of the simulations are presented in Section 3. Interpretations of the results are discussed in Section 4.

2. Model Formulation

The non-dimensional velocity field for the reduced system of equations for Langmuir circulation [26] is given by

$$\begin{aligned} u &= 1 + z - C(t)\cos\pi z - B(t)\cos l\pi y, \\ v &= A(t)\pi\cos\pi z\sin l\pi y \quad \text{and} \quad w = -A(t)l\pi\sin\pi z\cos l\pi y, \end{aligned} \tag{1}$$

where l is the aspect ratio of circulation depth (i.e., depth of the thermocline), D, to circulation width and the fluid velocity, $\mathbf{u} = (u,\ v,\ w)^T$, naturally satisfies the incompressibility condition, $\nabla\cdot\mathbf{u} = 0$. Figure 1 indicates the coordinate system and portrays the flow described by the equations, for which typical field measurements [2, 21] have been added. Both field observations [13, 21, 38] and theory [10, 26] give a critical windspeed of 3 m s^{-1}, above which Langmuir circulation is evident. For regions of parameter space for which steady states are stable, the steady states are given by

$$B = \frac{8A}{\pi^2 l(4 + A^2)} \qquad \text{and} \quad C = \frac{ABl}{2}\,, \tag{2}$$

where A is a parameter that represents the speed of the circulation and is a function of the eddy viscosity [20], ν_T, thermal diffusivity and the Stokes drift gradient [26] all of which are difficult to estimate or measure. For our purposes, A may be regarded as a parameter determined directly from observations. In order for us to do this, we require the dimensional variables given by

$$(\hat{y}, \hat{z}) = (y, z)D, \quad (\hat{v}, \hat{w}) = (v, w)\frac{\nu_T}{D}\,, \tag{3}$$

$$\hat{u} = u\frac{u_*^2 D}{\nu_T} \quad \text{and} \quad \hat{t} = t\frac{D^2}{\nu_T}\,, \tag{4}$$

where u_* is the water friction velocity determined by the applied wind stress, ρu_*^2, acting on a mass of fluid of density ρ.

The above description of a velocity field is from what is commonly called a Eulerian point-of-view, where the whole system is observed with respect to a fixed location. In some instances it is beneficial to follow a single "blob" of fluid, or a particle, through the flow and record its trajectory. From this Lagrangian perspective we study the dynamical system of the velocity field given by

$$\frac{\mathrm{d}}{\mathrm{d}t}\begin{pmatrix} x \\ y \\ z \end{pmatrix} = \begin{pmatrix} u(y,z) \\ v(y,z) \\ w(y,z) \end{pmatrix}. \tag{5}$$

The velocity field is independent of x and the cross-sectional velocities can be written in terms of a streamfunction, ϕ, as

$$v = \frac{\partial\phi}{\partial z} \quad \text{and} \quad w = -\frac{\partial\phi}{\partial y}\,, \tag{6}$$

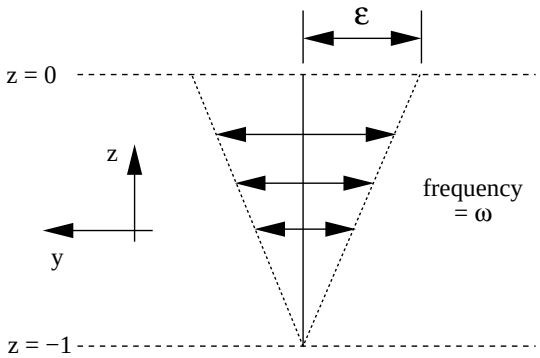

Figure 2. The time-dependent perturbation which is superimposed on the steady flow.

where

$$\phi = A \sin \pi z \sin l\pi y. \tag{7}$$

In this sense the flow is Hamiltonian (and integrable), with Hamiltonian ϕ, such that all the streamlines are closed and can be found explicitly. Clearly, in the absence of diffusion, an advected particle will remain on the closed orbit that it started on. To follow an individual particle with (positive or negative) buoyancy, V_s, we amend the above equations by putting

$$\frac{\mathrm{d}z}{\mathrm{d}t} = w(y, z) + V_s(z), \tag{8}$$

where we make sure that V_s goes rapidly to zero at the upper boundary to avoid the possibility of particles leaving the upper surface. The incompressibility condition is also satisfied for the trajectories of buoyant particles in the main body of the fluid flow where the buoyancy is roughly constant. Particle inertia may also play a role in this system due to the differences between particle and fluid density. If the circulation is sufficiently large and slow this effect may be quantitatively insignificant, however, it may make large qualitative differences. In particular, the particle trajectories will no longer satisfy the incompressibility condition, indicating that particle aggregations may occur. This will also be the case for specific active strategies adopted by the plankton. We do not deal with these issues explicitly in this paper.

Real flows in the sea are unlikely to be as perfect as the above description suggests. Therefore, to investigate the effects of small time-dependent variations, we consider a small amplitude fluctuation of the flow perpendicular to the direction of the wind such that the flow is unchanged at $z = -1$ (see Figure 2). This is obtained by the transformation

$$y \longrightarrow y + \varepsilon g(t)(z + 1), \tag{9}$$

where $g(t)$ is the time-periodic forcing function given by

$$g(t) = \sin \omega t. \tag{10}$$

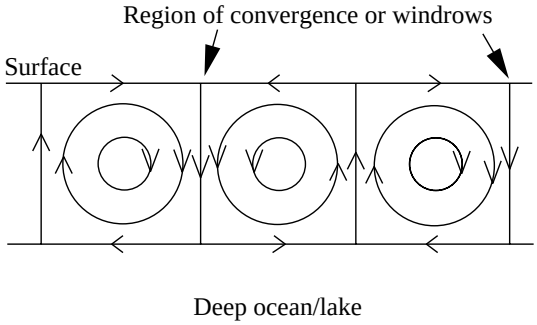

Figure 3. Steady cross-sectional streamlines for neutrally buoyant particles.

To first order in ε, the streamfunction becomes

$$\psi_\varepsilon = A \sin \pi z \sin l\pi y + \varepsilon A g(t) l\pi (z+1) \sin \pi z \cos l\pi y \tag{11}$$

which defines a very similar flow to the full streamfunction and, hence, we will use the above truncation throughout the remainder of the paper. The above system is similar to the "even" oscillatory instability for Rayleigh–Bénard convection as studied by [7] and many of the techniques that they employ can be used here (e.g., Melnikov theory can be used to analytically investigate the spread of plankton). Notably, we make important distinctions in the application and interpretation of the results.

3. Simulation

A simple 4th-order Runge–Kutta scheme is used to integrate the three ordinary differential equations. We note, however, that the results as presented here are insensitive to the particular numerical scheme used.

As mentioned previously, the streamlines for neutrally buoyant particles in a steady flow are closed and, in the absence of any diffusive processes, particles stay on the streamlines for all time. This scenario is depicted in Figure 3. The cross-sectional streamlines for positively buoyant particles in a steady flow are displayed in Figure 4 where it is clear that there are two qualitatively different behaviours for particles: some particles are trapped in closed orbits some distance below the surface whereas others accumulate at the point (or line when also considering the longitudinal flow) of convergence of streamlines at the fluid surface. There is a clear, smooth boundary between these two regions. The set of closed orbits form what is called a Stommel retention zone (after Stommel [35, 36]). In the absence of any other transport or diffusive processes, buoyant particles that begin at the surface cannot submerge due to the upward vertical component of the buoyant particle trajectories (Figure 4) and, hence, will never enter the Stommel retention zone no matter how fast the fluid flow is in the Langmuir circulation (in contrast to the conclusions of [42]).

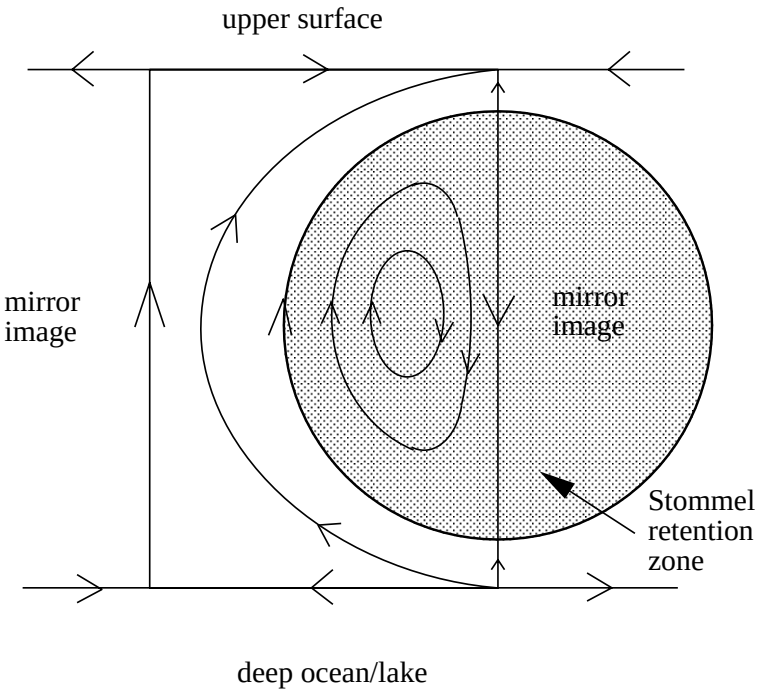

Figure 4. Steady cross-sectional streamlines for particles of positive buoyancy. Above the Stommel retention zone, all trajectories have a vertical component which points upwards. Therefore, no positively buoyant particles can move downwards from the upper surface no matter how strong the Langmuir circulation. The shaded region indicates a region of closed streamlines and is called a Stommel retention zone.

Upon adding a small time-dependent perturbation to the flow, the clear boundaries between the regions evaporate. Consider the streamfunction given by Equation (11) for an unsteady flow field. To simplify the analysis, we calculate the Poincaré section; we record the position of an advected particle at times t when the forcing function, $g(t)$, is zero (i.e., at times, $t = 0, (2\pi)/\omega, \ldots, (2n\pi)/\omega$, where n is an integer). A good way to measure how much the time-dependent perturbation affects the trajectory of a particle is to calculate the particles "escape time", or the value of n for which a particle first leaves the Langmuir cell that it started in. Figures 5 to 7 display the escape time as a function of the particles initial condition within a single Langmuir cell. In contrast to the steady velocity field, particles are not necessarily constrained to closed orbits and can wander through the whole space. In particular, for the non-autonomous system, trajectories can cross. There are no clear boundaries between regions of varying escape times and, in fact, the boundaries are fractal in nature. The dark regions in Figures 5 to 7 indicate that the particle never leaves the Langmuir cell and, in this paper, we label these regions "retention zones". By varying the frequency of the unsteady perturbation the structure of the escape space changes dramatically. Increasing the

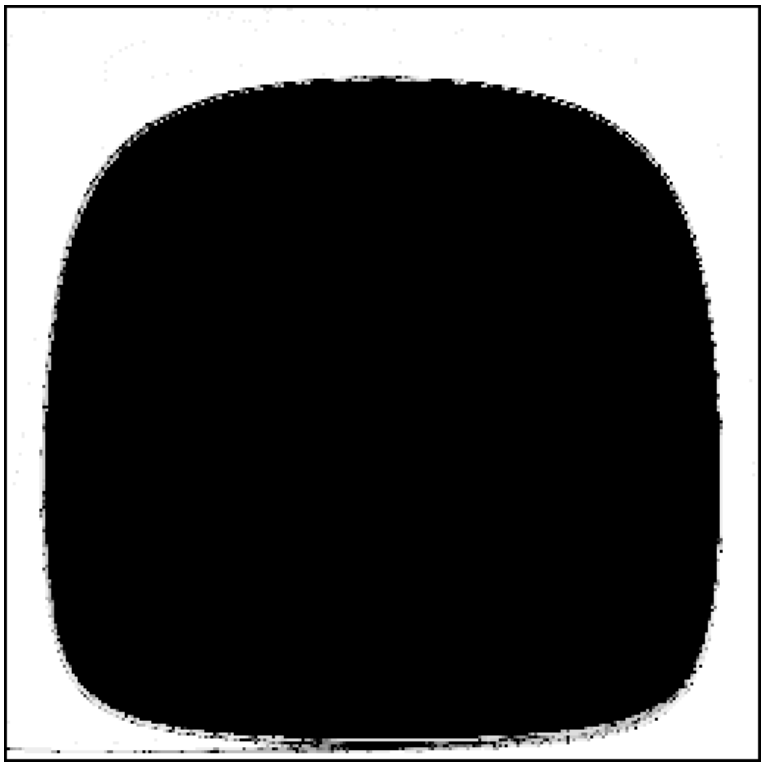

Figure 5. Escape times for neutrally buoyant advected particles whose initial cross-sectional positions are plotted. The greyscale indicates the number of oscillations required before the particle leaves the Langmuir cell, where white represents one oscillation and black represents more than 100 oscillations. The circulation speed, A, and the perturbation amplitude, ε, both equal 0.1 and the forcing frequency, ω, equals 0.3.

frequency from $\omega = 0.3$ (Figure 5) to $\omega = 0.6$ (Figure 6) reduces the size of the "central retention zone" but introduces extra "resonant retention zones". These resonant retention zones are advected with the flow but remain separate from the surrounding fluid. In Figure 8 we plot the cross-sectional positions of a uniform grid of neutrally buoyant particles after 50 forcing oscillations ($n = 50$) allowing particles to escape from the Langmuir cell. No particles were allowed to enter the Langmuir cell from elsewhere, but a similar picture was obtained when particles were allowed to re-enter the Langmuir cell. There are clear regions which exhibit coherent behaviour and have been left behind after approximately half the initial number of particles have escaped. The coherent behaviour is even more evident when we also consider the longitudinal displacement as a function of the particles' initial conditions, as shown in Figure 9. Particles in the retention zones, on average, all travel at the same longitudinal speed whereas particles in the mixed, or chaotic, regions are widely dispersed in the longitudinal direction. All the figures clearly show the stretching and folding that occurs on the boundaries of the coherent

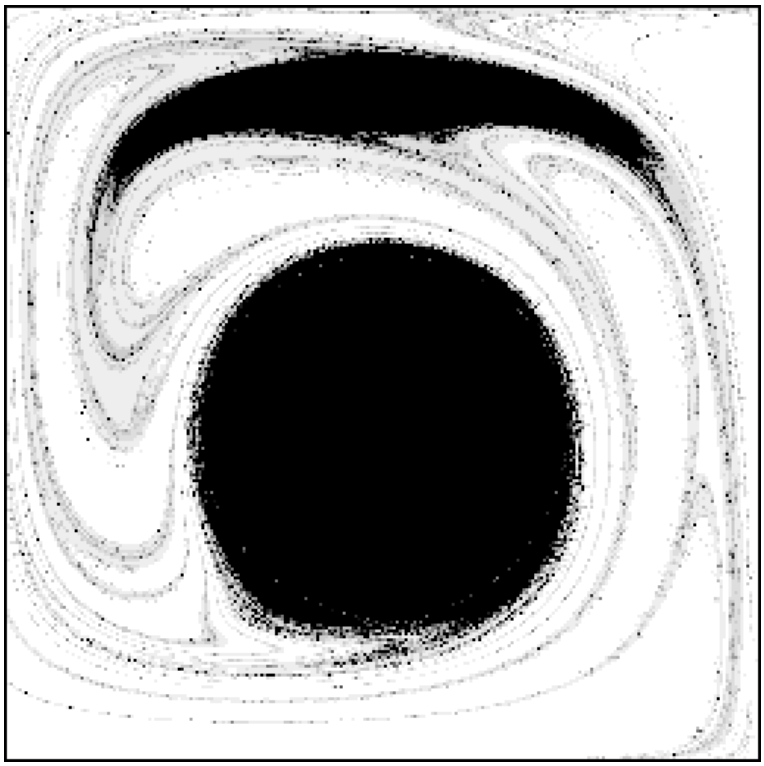

Figure 6. Escape times for neutrally buoyant advected particles whose initial cross-sectional positions are plotted. The greyscale indicates the number of oscillations required before the particle leaves the Langmuir cell, where white represents one oscillation and black represents more than 100 oscillations. The circulation speed, A, and the perturbation amplitude, ε, both equal 0.1 and the forcing frequency, ω, equals 0.6.

regions. Increasing the forcing frequency further to $\omega = 1.2$ (Figure 7) we see that the central retention zone decreases in size again but higher order resonant retention zones are produced. A graph of the sum of the relative area of the retention zones, compared to total area, is plotted in Figure 10. It is clear that there is a minimum value of the relative retention zone area corresponding to a forcing frequency of approximately $\omega = 0.75$. The resonant retention zones persist for as long as the physical forcing remains constant. The escape times for positively buoyant particles (i.e., $V_s > 0$) are displayed in Figures 11 and 12 in which we keep the same forcing frequency as in Figure 6 (i.e., $\omega = 0.6$). The asymmetry can be clearly seen and, in general terms, the regions adopt the structure of Figure 4. The figures also share characteristics from Figure 6, and it is evident that the total area of the retention zones in Figures 11 and 12 are less than the area of the corresponding Stommel retention zones for the steady flow. Again, resonant retention zones are produced that revolve around the central retention zone.

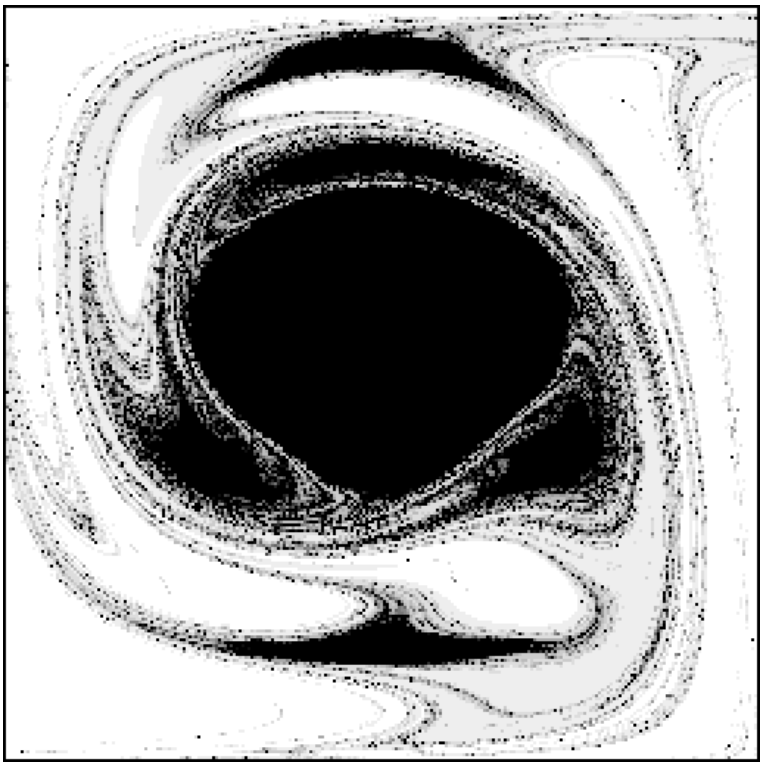

Figure 7. Escape times for neutrally buoyant advected particles whose initial cross-sectional positions are plotted. The greyscale indicates the number of oscillations required before the particle leaves the Langmuir cell, where white represents one oscillation and black represents more than 100 oscillations. The circulation speed, A, and the perturbation amplitude, ε, both equal 0.1 and the forcing frequency, ω, equals 1.2.

4. Conclusion

We can apply Melnikov theory to this problem and extract a measure of the size of the coherent regions theoretically [40]. It is also possible to calculate an estimate of the heteroclinic lobes and, hence, quantify the transport and effective diffusivity of plankton due to the forcing [7]. However, due to the rather arbitrary nature of the time-dependent perturbation, we refrain from doing that in this paper and concentrate on the qualitative interpretation. The result of resonance between two types of physical forcing is to provide additional retention zones, which are advected with the flow and do not diminish in size. The retention zones consist of regions of coherent flow that are isolated in regions of chaotic behaviour. Longitudinal transport of the retention zones is also coherent and the plankton are given the opportunity to be surrounded by organisms of the same species. Given sufficient time, this may enable them to mate sexually and form high local concentrations. Field studies also report the presence of coherent patches, on a variety of scales, that are not destroyed by an otherwise turbulent velocity field [6, 12, 15, 22, 28, 29, 37, 41, 39].

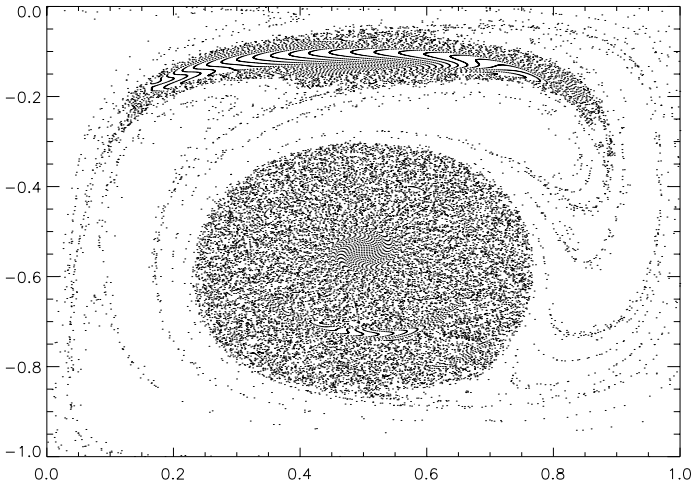

Figure 8. Distribution of neutrally buoyant particles, after 50 oscillations with a forcing frequency of $\omega = 0.6$, from a regular grid of particles occupying the space of one Langmuir roll. Here, plankton are allowed to escape from the region defined by $y \in [0, 1]$. Coherent regions of space can be observed as can regions where particles are quickly removed. $A = \varepsilon = 0.1$ with 256^2 pixels.

There are clear regions where phytoplankton tend to stay in the same patches, as can be seen in Figures 5 to 8, and regions where much mixing is evident, both in the cross-sectional space and longitudinally (Figure 9). The transport of particles in the chaotic regions is potentially much quicker than for molecular (or swimming) diffusion alone, as particles a small distance apart can move to adjacent Langmuir cells after only one period. Regions where particle trajectories can deviate quickly are clearly seen, particularly close to the circulation boundaries due to the complex structure of the heteroclinic connection. This is in contrast to particles that start in the coherent regions where the structure is clear. Beginning with a patch of plankton of a similar length-scale to the Langmuir roll, plankton in the chaotic regions are quickly removed from the system and a skeleton of plankton is left behind in the coherent regions. The coherent regions are different for particles of varying buoyancy (see Figures 11 and 12). In general, increasing the magnitude of the buoyancy of the particles decreases the size and changes the location of the coherent regions. Therefore, different species of phytoplankton with dissimilar buoyancy will form patches in a variety of locations and, hence, zooplankton must be able to adapt to locate and follow different prey efficiently. It is also likely that phytoplankton can adjust their buoyancy over a short time-scale in response to the available light source [25] and, hence, phytoplankton could escape a coherent light-deficient patch by changing their buoyancy. This could result in the organism's

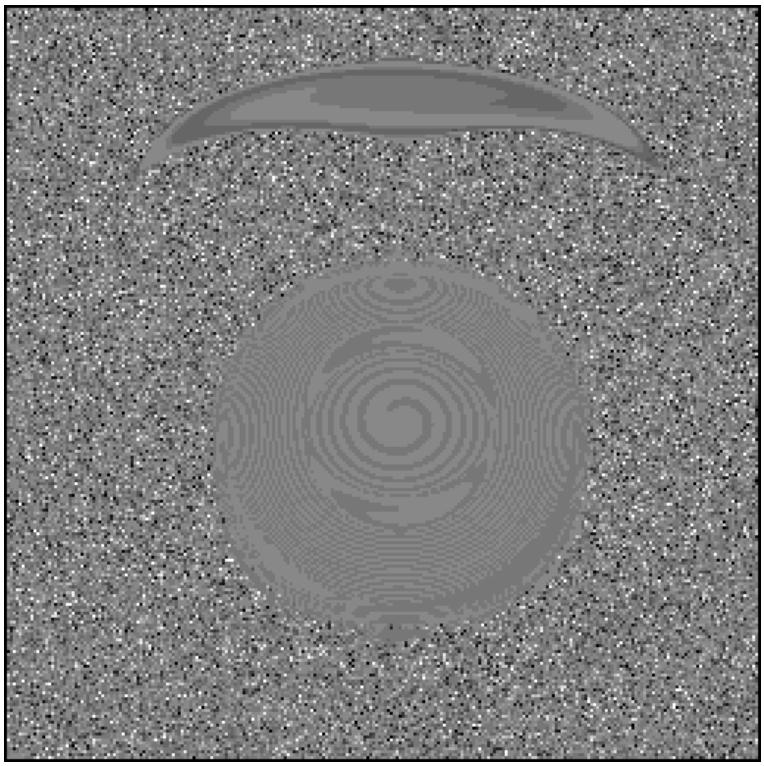

Figure 9. Longitudinal displacement of particles that start from $x = 0$ at a given cross-sectional location. The linear greyscale portrays the longitudinal distance travelled, where white indicates the largest distance and black indicates zero. $A = \varepsilon = 0.1$ and $\omega = 0.6$ with 256^2 pixels.

local environment effectively changing into a chaotic region, thus allowing it to harness the chaotic region's transport and mixing dynamics.

The upshot of the difference in buoyancy between phytoplankton and purely advected particles is that their retention zones differ (i.e., the trajectories of the positively buoyant phytoplankton that get trapped in the retention zones of Figure 12 will intersect the trajectories of neutrally buoyant particles in the chaotic regions of Figure 6). This enables the phytoplankton to have a fresh mixed supply of essential nutrients.

The effect of particle inertia (due to the possible difference in densities of the fluid and the particle) may not appear significant for large, slowly moving Langmuir circulations but qualitatively the system may be very different. The fluid trajectories may no longer be incompressible and this would allow aggregations of particles to occur. This will be investigated in detail in a later paper. Also, zooplankton are able to change their swimming characteristics in response to the availability of prey and their vulnerability to higher predators [11, 17, 27]. Depending on the zooplankton's feeding characteristics, living in a chaotic region

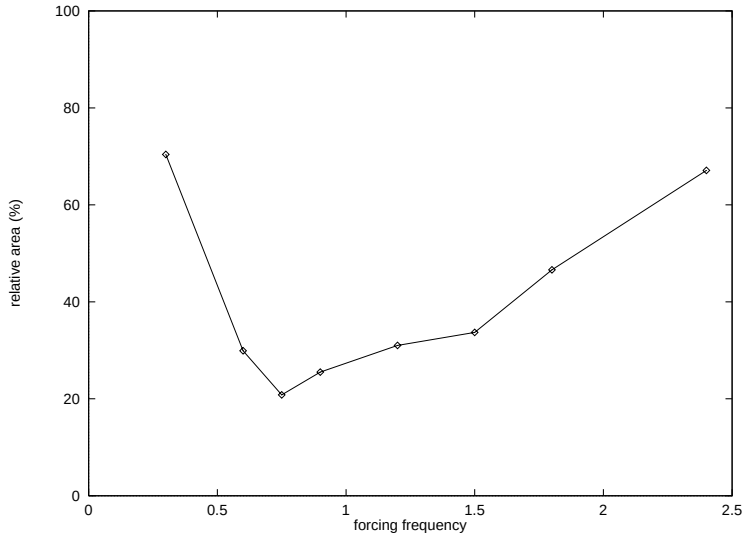

Figure 10. A plot of the numerically computed values for the relative area of the retention zones, with respect to the total area. The diamonds indicate data points and the lines are for illustration.

may either be beneficial or detrimental [32]. For filter feeders that do not swim and wait for prey to come close, the chaotic region has the effect of increasing encounter rates with phytoplankton. However, for a predator that actively pursues prey, the diverging flow trajectories could prove difficult to traverse, thus decreasing its capacity for successful capture. To leave the chaotic regions, zooplankton must change their effective buoyancy (i.e., swimming up or down) until the prey are encountered in the coherent region (similar to [11], but transport of zooplankton can occur at much greater speeds making use of the flow than for swimming alone). It would obviously be beneficial for zooplankton to remain in this region until the foodsource has run out or if they get chased by larger predators and, therefore, they should match the buoyancy of the phytoplankton. Thus, zooplankton may make use of the chaotic regions to move swiftly and economically between phytoplankton coherent regions and to evade predators [43]. To do this they could make use of the light intensity and adjust their buoyancy accordingly.

In open oceans and lakes, it is likely that there will be significant variations in windspeed and illumination which may influence the overall structure of the Langmuir circulation. Also, factors such as variations in transversal current and wind shear stress may alter the internal retention zone structure of the Langmuir circulation by a corresponding variation in the forcing frequency. It is the timescales of these variations that are important for the construction and maintenance of the resonant retention zones. One can imagine a smooth transition between Figures 5 to 7 for which certain retention zones would persist throughout the process but others

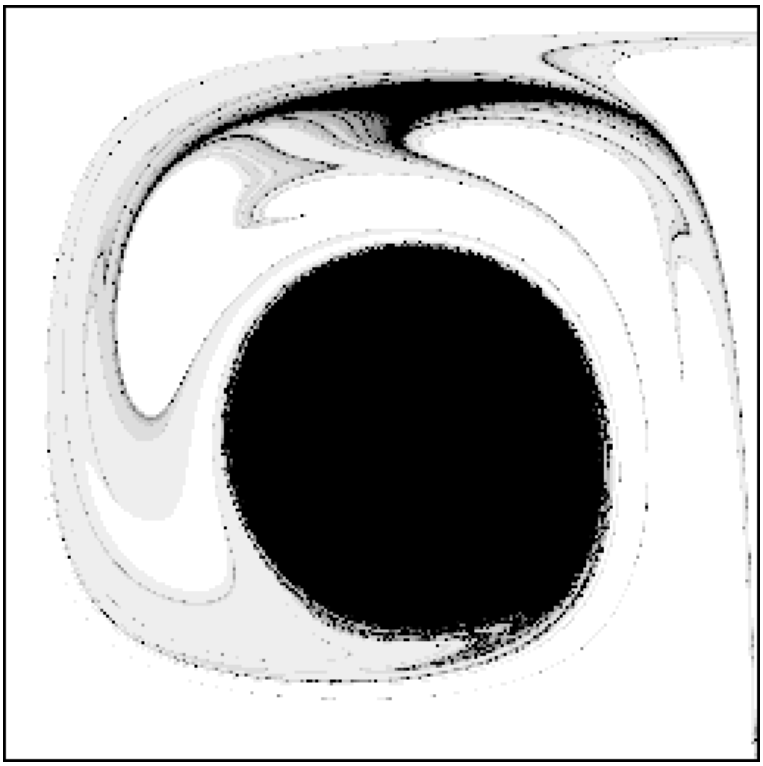

Figure 11. Escape times for positively buoyant ($V_s = 0.032$) advected particles whose initial cross-sectional positions are plotted. The greyscale indicates the number of oscillations required before the particle leaves the Langmuir cell, where white represents one oscillation and black represents more than 100 oscillations. The circulation speed, A, and the perturbation amplitude, ε, both equal 0.1 and the forcing frequency, ω, equals 0.6.

would exist for relatively short periods of time. We indicate the relative areas of these coherent regions in Figure 10.

Variations of light and wind lead to a path in the parameter space of the dynamical system derived by Moroz and Leibovich [26] and present the possibility of oscillatory solutions as well as steady solutions. Cox et al. [8, 9] demonstrate the existence of a whole range of solutions, which can co-exist, such as steady, oscillatory and multiple oscillatory states. They find, however, "that the only robustly observable motions that should be anticipated are travelling waves and steady states". Also, they report the existence of transversally drifting Langmuir circulations in field studies and indicate that stable stratification "causes the most unstable (linear) modes to rotate from the wind direction", although this is only a minor affect. What we conclude from these studies is that a whole host of instabilities arise from the model irrespective of other arbitrary external forcing. It is expected that some of these oscillatory modes will exhibit similar behaviour to the system described in this paper.

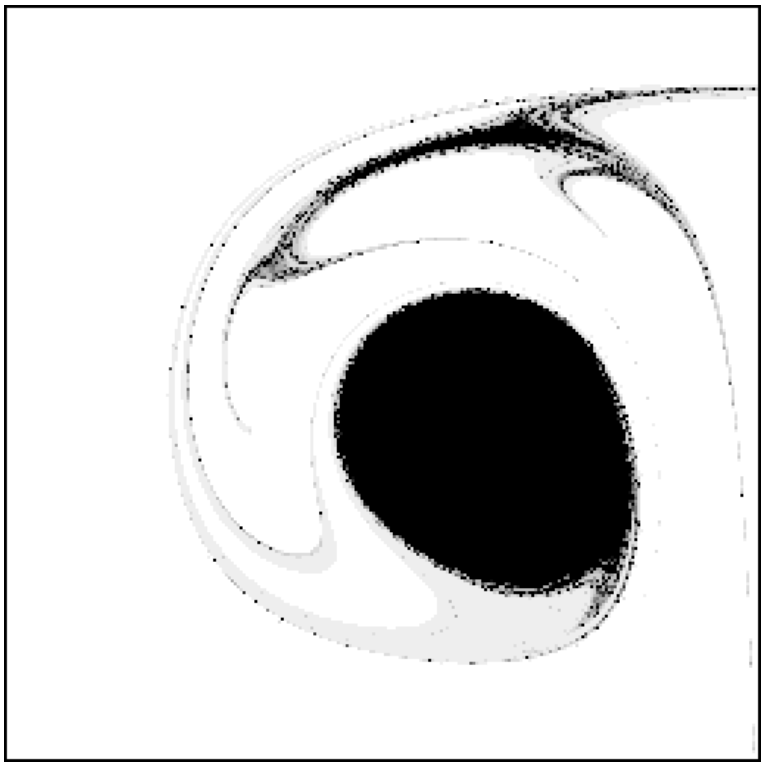

Figure 12. Escape times for positively buoyant ($V_s = 0.1$) advected particles whose initial cross-sectional positions are plotted. The greyscale indicates the number of oscillations required before the particle leaves the Langmuir cell, where white represents one oscillation and black represents more than 100 oscillations. The circulation speed, A, and the perturbation amplitude, ε, both equal 0.1 and the forcing frequency, ω, equals 0.6.

If the Langmuir circulation slows down and stops it will leave behind patches that may diffuse relatively slowly due to turbulence but this could be balanced by the active aggregation of plankton [11]. Therefore, the patches may persist in the absence of Langmuir circulation and may even be entrained in the flow if the circulation restarts. Some patches will be positioned within the coherent regions and others not and so some patches will remain and others will quickly disappear. This may indeed benefit one species with a particular buoyancy and not another, but this would depend explicitly on the physical conditions.

The effect of other diffusive processes on the unsteady flow (such as turbulence) may do no more than blur the edges of the retention zones enabling particles to diffuse in and out. However, it has been shown by [11] that by including the effects of the swimming behaviour of the plankton (see also [5, 16, 30]) as a biological diffusivity, the plankton trajectories are no longer incompressible and plankton can actively aggregate. This may help plankton to accumulate in areas beneficial to

them (such as, perhaps, the coherent regions), and is an obvious extension to the above work.

Acknowledgments

I thank Professor J. McGlade, Dr. I. Mezic and Professor D. Rand for their input and financial support for this work.

References

1. Arnold, V.I., *Mathematical Methods of Classical Mechanics*, 2nd edition. Springer-Verlag, Berlin, 1989.
2. Barstow, S.F., The ecology of Langmuir circulation: A review. *Marine Environmental Research* **9** (1983) 211–236.
3. Bees, M.A., Non-linear pattern generation in suspensions of swimming micro-organisms. Ph.D. Thesis, University of Leeds (1996).
4. Bees, M.A. and Hill, N.A., Wavelengths of bioconvection patterns. *Journal of Experimental Biology* **200** (1997) 1515–1526.
5. Bees, M.A., Hill, N.A. and Pedley, T.J., Analytical approximations for the orientation of small dipolar particles in steady shear flows. *Journal of Mathematical Biology* **36** (1998) 269–298.
6. Benfield, M.C., Davis, C.S., Wiebe, P.H., Gallager, S.M., Lough, R.G. and Copley, N.J., Video plankton recorder estimates of copepod, pteropod and larvacean distributions from a stratified region of Georges Bank with comparative measurements from a MOCNESS sampler. *Deep-Sea Research Part II – Topical Studies in Oceanography*, **43**(7–8) (1996) 1925–1945.
7. Camassa, R. and Wiggins, S., Chaotic advection in a Rayleigh–Bénard flow. *Physical Review A* **43**(2) (1991) 774–797.
8. Cox, S.M., Leibovich, S., Moroz, I.M. and Tandon, A., Nonlinear dynamics in Langmuir circulations with O(2) symmetry. *Journal of Fluid Mechanics* **241** (1992) 669–704.
9. Cox, S.M., Leibovich, S., Moroz, I.M. and Tandon, A. Hopf bifurcations in Langmuir circulations. *Physica D* **59** (1992) 226–254.
10. Craik, A.D.D. and Leibovich, S., A rational model for Langmuir circulations. *Journal of Fluid Mechanics* **73** (1976) 401–426.
11. Davis, C.S., Flierl, G.R., Wiebe, P.H. and Franks, P.J.S., Micropatchiness, turbulence and recruitment in plankton. *Journal of Marine Research* **49** (1991) 109–151.
12. Denman, K.L. and Herman, A.W., Space-time structure of a continental shelf ecosystem measured by a towed porpoising vehicle. *Journal of Marine Research* **36** (1978) 693–714.
13. Faller, A.J. and Woodcock, A.H., The spacing of windrows of *Sargassum* in the ocean. *Journal of Marine Research* **22** (1964) 22–29.
14. Gallager, S.M., Davis, C.S., Epstein, A.W., Solow, A. and Beardsley, R.C., High-resolution observations of plankton spatial distributions correlated with hydrography in the Great South Channel, Georges Bank. *Deep-Sea Research Part II – Topical Studies in Oceanography* **43**(7–8) (1996) 1627–1663.
15. Haury, L.R. and Wiebe, P.H., Fine-scale multi-species aggregations of oceanic zooplankton. *Deep Sea Research* **29** (1982) 915–921.
16. Hill, N.A. and Häder, D.P., A biased random walk model for the trajectories of swimming micro-organisms. *Journal of Theoretical Biology* **186** (1997) 503–526.
17. Hunter, J.R. and Thomas, G.L., Effect of prey distribution on the searching and feeding behaviour of larval anchovy *Engraulis mondax Girard.* In: Blaxter, J.H.S. (ed.), *The Early Life History of Fish*. Springer-Verlag, New York (1974) p. 559.

18. Jones, S.W. and Young, W.R., Shear dispersion and anomalous diffusion by chaotic advection. *Journal of Fluid Mechanics* **280** (1994) 149–172.
19. Langmuir, I., Surface motion of water induced by wind. *Science* **87** (1938) 119–123.
20. Leibovich, S., Convective instability of stably stratified water in the ocean. *Journal of Fluid Mechanics* **82** (1997) 561–581.
21. Leibovich, S., The form and dynamics of Langmuir circulations. *Annual Review of Fluid Mechanics* **15** (1983) 391–427.
22. Lenz, J., Schnack, D., Petersen, D., Kreikemeier, J., Hermann, B., Mees, S. and Wieland, K. The ichthyoplankton recorder – A video recording-system for in-situ studies of small-scale plankton distribution patterns. *ICES Journal of Marine Science* **52**(3–4) (1995) 409–417.
23. Malchow, H., Spatio-temporal pattern formation in non-linear nonequilibruim plankton dynamics. *Proceedings of the Royal Society of London, B* **251** (1993) 103–109.
24. Malchow, H., Non-linear plankton dynamics and pattern formation in an ecohydrodynamic model system. *Journal of Marine Systems* **7** (1996) 193–202.
25. Moore, J.K. and Villareal, T.A., Buoyancy and growth-characteristics of 3 positively buoyant marine diatoms. *Marine Ecology-Progress Series* **132**(1–3) (1996) 203–213.
26. Moroz, I.M. and Leibovich, S., Competing instabilities in a nonlinear model of Langmuir circulations. *Physics of Fluids* **28** (1985) 2050–2061.
27. Munk, P., Foraging behaviour of larval cod (*Gadus morhua*) influenced by prey density and hunger. *Marine Biology* **122**(2) (1995) 205–212.
28. Owen, R.W., Microscale patchiness in the larval anchovy environment. *Rapp. Proces. Verb. Reun. Cons. Int. Explor. Mer. Res.* **178** (1981) 364–368.
29. Owen, R.W., Microscale and finescale variations of small plankton in coastal and pelagic environments. *Journal of Marine Research* **47** (1989) 197–240.
30. Pedley, T.J. and Kessler, J.O., Hydrodynamic phenomena in suspensions of swimming microorganisms. *Annual Review of Fluid Mechanics* **24** (1992) 313–358.
31. Pinelalloul, B., Spatial heterogeneity as a multiscale characteristic of zooplankton community. *Hydrobiologia* **301** (1995) 17–42.
32. Saiz, E. and Kiorboe, T., Predatory and suspension feeding of the copepod *Acartia tonsa* in turbulent environments. *Marine Ecology-Progress Series* **122** (1995) 147–158.
33. Solow, A. and Steele, J.H., Scales of plankton patchiness – Biomass versus demography. *Journal of Plankton Research* **17**(8) (1995) 1669–1677.
34. Spiegel, E.A. and Zaleski, S., Reaction-diffusion instability in a sheared medium. *Physics Letters* **106A**(7) (1984) 335–338.
35. Stommel, H., Trajectories of small bodies sinking slowly through convection cells. *Journal of Marine Research* **8** (1949) 24–29.
36. Stommel, H., Streaks on natural water surfaces. *Weather* **6** (1951) 72–74.
37. Visman, V., Mcqueen, D.J. and Demers, E., Zooplankton spatial patterns in 2 lakes with contrasting fish community structure. *Hydrobiologia* **284**(3) (1994) 177–191.
38. Walther, E.G., Wind streaks. MSc Thesis, State University of New York, Albany (1967).
39. Wiafe, G. and Frid, C.L.J., Short-term temporal variation in coastal zooplankton communities: The relative importance of physical and biological mechanisms. *Journal of Plankton Research* **18** (1996) 1485–1501.
40. Wiggins, S., *Introduction to Applied Non-Linear Dynamical Systems and Chaos*. Springer-Verlag, New York, 1990.
41. Wishner, K.F., Schoenherr, J.R., Beardsley, R. and Chen, C.S., Abundance, distribution and population-structure of the copepod *Calanus finmarchicus* in a springtime right-whale feeding area in the southwestern Gulf of Maine. *Continental Shelf Research* **15**(4–5) (1995) 475–507.
42. Woodcock, A.H., Winds subsurface pelagic *Sargassum* and Langmuir circulations. *Journal of Experimental Marine Biology and Ecology* **170** (1993) 117–125.

43. Yen, J. and Strickler, J.R., Advertisement and concealment in the plankton – What makes a copepod hydrodynamically conspicious. *Invertebrate Biology* **115**(3) (1996) 191–205.
44. Yool, A.J., The dynamics of open-ocean plankton ecosystem models. Ph.D. Thesis, University of Warwick (1998).